NASA TECHNICAL NOTE

NASA TN D-5787

NASA TN D-5787

A SMALL BALLISTIC RANGE FOR IMPACT METAMORPHISM STUDIES

by Friederich Hörz

Ames Research Center
Moffett Field, Calif. 94035

NATIONAL AERONAUTICS AND SPACE ADMINISTRATION • WASHINGTON, D. C. • MAY 1970

1. Report No.	2. Government Accession No.	3. Recipient's Catalog No.
NASA TN D-5787		

4. Title and Subtitle	5. Report Date
A SMALL BALLISTIC RANGE FOR IMPACT METAMORPHISM STUDIES	May 1970
	6. Performing Organization Code

7. Author(s)	8. Performing Organization Report No.
Friederich Hörz	A-3181
	10. Work Unit No.
	129-03-16-02-00-21

9. Performing Organization Name and Address	11. Contract or Grant No.
NASA Ames Research Center Moffett Field, California 94035	
	13. Type of Report and Period Covered
12. Sponsoring Agency Name and Address	Technical Note
National Aeronautics and Space Administration Washington, D.C. 20546	14. Sponsoring Agency Code

15. Supplementary Notes

16. Abstract

This paper describes the design and operation of a ballistic range capable of shock loading rocks and minerals to precisely known pressures.

The projectile is accelerated by conventional gunpowder and launched in a 20-mm gun barrel. A system of He/Ne lasers and photodiodes in combination with three X-ray flash tubes permits accurate timing. The response time of this system is less than 10^{-6} sec. X-ray shadow photographs are superimposed on a precise fiducial grid, which monitors possible projectile tilt. The maximum velocities obtained to date are 3.2 km/sec.

The maximum pressures achievable in various geological materials range from 250-500 kb, depending on the respective densities of the target and the projectile. These pressures cover a wide range of solid state reactions that are of special interest for the study of impact-metamorphism, as illustrated by some results obtained from the study of shock-loaded single crystals of quartz.

Cleavage in quartz is produced by shock pressures as low as 50 kb and develops predominantly on crystallographic planes with high resolved shear stress. Planar features develop at pressures above 100 kb and cluster near $\{10\bar{1}3\}$ regardless of impact direction; at pressures above 160 kb, they develop strongly on $\{10\bar{1}2\}$. Refractive index measurements indicate that the breakdown of the quartz lattice to an amorphous state occurs gradually over a pressure range from about 200 to 300 kb. Above 300 kb the breakdown of the quartz lattice is essentially complete.

17. Key Words (Suggested by Author(s))	18. Distribution Statement
Impact shock Experimental shock facility High pressure	Unclassified - Unlimited

19. Security Classif. (of this report)	20. Security Classif. (of this page)	21. No. of Pages	22. Price*
Unclassified	Unclassified	18	$3.00

*For sale by the Clearinghouse for Federal Scientific and Technical Information
Springfield, Virginia 22151

A SMALL BALLISTIC RANGE FOR IMPACT METAMORPHISM STUDIES[1]

Friederich Hörz

Ames Research Center

SUMMARY

This paper describes the design and operation of a ballistic range capable of shock loading rocks and minerals to precisely known pressures.

The projectile is accelerated by conventional gunpowder and launched in a 20-mm gun barrel. A system of He/Ne lasers and photodiodes in combination with three X-ray flash tubes permits accurate timing. The response time of this system is less than 10^{-6} sec. X-ray shadow photographs are superimposed on a precise fiducial grid, which monitors possible projectile tilt. The maximum velocities obtained to date are 3.2 km/sec.

The maximum pressures achievable in various geological materials range from 250-500 kb, depending on the respective densities of the target and the projectile. These pressures cover a wide range of solid state reactions that are of special interest for the study of impact metamorphism, as illustrated by some results obtained from the study of shock-loaded single crystals of quartz.

Cleavage in quartz is produced by shock pressures as low as 50 kb and develops predominantly on crystallographic planes with high resolved shear stress. Planar features develop at pressures above 100 kb and cluster near $\{10\bar{1}3\}$ regardless of impact direction; at pressures above 160 kb, they develop strongly on $\{10\bar{1}2\}$. Refractive index measurements indicate that the breakdown of the quartz lattice to an amorphous state occurs gradually over a pressure range from about 200 to 300 kb. Above 300 kb the breakdown of the quartz lattice is essentially complete.

INTRODUCTION

Recent interest in the morphology and origin of the lunar surface features has stimulated detailed investigations of terrestrial meteorite craters, thus creating an important new field in geology. Problems in connection with the identification of terrestrial impact craters in various stages of erosion are complex and involve structural fieldwork as well as detailed mineralogic and petrographic studies. Because the structural evidence obtained by field studies is subject to various interpretations, the most widely accepted criterion of an impact origin is the presence of unique microdeformations and high pressure forms of component mineral grains, both of which are unknown from any other terrestrial geologic events.

[1]The author performed this work while on tenure as a National Research Council-National Academy of Sciences Postdoctoral Research Associate.

While the high pressure polymorphs require high peak pressures for their formation, only the microdeformations appear to occur exclusively under very high dynamic stress and strain rates, which presumably are produced by the passage of a shock wave generated by an impacting meteorite. The process giving rise to these products has been termed "shock metamorphism." Various petrologists have established an empirical sequence of increasing shock damage intensity, termed "stages of increasing shock metamorphism," but they could relate these stages only approximately to peak pressures and temperatures (refs. 1 through 11).

It is possible to simulate the natural impact conditions in the laboratory by making use of methods developed in the study of very high pressure physics (refs. 12 through 17). Rocks and single crystals can be shock loaded to precisely known peak pressures, and the products of controlled experiments can be correlated with the pressure-temperature history of the recovered samples. The information thus gained permits a more quantitative petrological interpretation of naturally shocked materials.

Various techniques are available for the shock loading of solids. All these techniques involve accelerating a "driver" plate against a "target" plate at very high velocities, thus producing a shock wave in the test material. The technique used at Ames Research Center, and described in this report, employs a conventional powder gun of 20-mm caliber as the accelerating mechanism. The experimental facility is capable of shock loading rocks and minerals to peak pressures in the range of 250-500 kb, depending on the projectile and target densities. Although these pressures are less than those produced by other experimental techniques or those occurring during natural events, the important solid state transformations that take place in this pressure range can be studied effectively under carefully controlled conditions as illustrated by the preliminary results reported here.

PRESSURE CALCULATION

Upon impact, the projectile (driver plate) produces a shock wave in both the projectile and target. With regard to pressure, density, and internal energy, these waves are virtually mathematical discontinuities and travel through the medium at supersonic velocities based on their normal speeds of sound at atmospheric conditions. The magnitude of these velocities and pressures suggest that the solids are in a fluid state.

The classical laws of conservation of mass flux (eq. (1)), momentum (eq. (2)), and energy (eq. (3)) are used to describe the relations of pressure (P), density (d), shock-wave velocity (U_s), particle velocity (u_p), and internal energy (E) in front of (o) and immediately behind (i) the shock front:

$$d_o U_s = d_i (U_s u_p) \tag{1}$$

$$P_i - P_o = d_o(U_s u_p) \tag{2}$$

$$P_i u_{pi} = \frac{1}{2}\left(d_o U_s\right)u_p^2 + d_o U_s\left(E_i - E_o\right) \tag{3}$$

The velocities are measured relative to the undisturbed material, assuming one-dimensional flow. From equations (1) and (2), one derives the basic "equation of state":

$$E_i - E_o = \frac{1}{2}\left(P_i + P_o\right)\left(V_o - V_i\right) \tag{4}$$

where the specific volume $V = 1/d$. The graphical presentation of equation (4) in the PV plane is called the "Hugoniot curve" of a solid. If one knows any two of the five parameters P, d, U_s, u_p, and E, all others can be calculated from the above equations. Since it is difficult or impossible to measure pressure, density, and internal energy directly, the most common method of obtaining a solution for equations (1), (2), and (3) is to measure U_s and u_p, either directly or indirectly. The pressure P_i is then calculated from equation (2), assuming $P_i >> P_o$:

$$P_i = d_o\left(U_s u_p\right) \tag{5}$$

Since the shock waves transmitted to the target and projectile on impact must satisfy the equations of state for both materials, it follows that at their interface

$$P_{i_{(\text{projectile})}} = P_{i_{(\text{target})}}$$

If one uses identical materials for both projectile and target, the generated shock waves are identical. The velocity of the projectile (V_p) is actually the particle velocity immediately before impact; therefore $V_p = 2u_p$. A technique commonly used to establish equations of state takes advantage of these relationships, requiring only measurements of projectile velocity and U_s in the target.

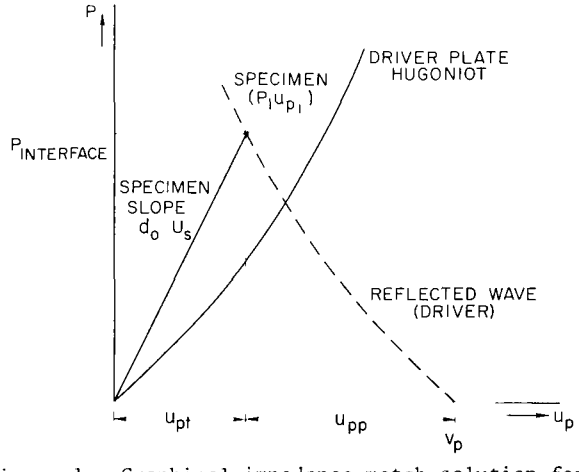

Figure 1.- Graphical impedance match solution for determining the pressure and particle velocity in target material for which the equation of state is unknown. The equation of state of the driver plate is known and V_p and U_{ST} must be measured.

This is a special case of the general law:

$$V_p = u_{p_{(\text{projectile})}} + u_{p_{(\text{target})}}$$

However, with a projectile of known equation of state and measurements of V_p and U_{st}, it is possible to obtain u_{pt} and the pressure in a target with an unknown Hugoniot equation of state by a graphical impedance match solution (fig. 1). The intersection of the

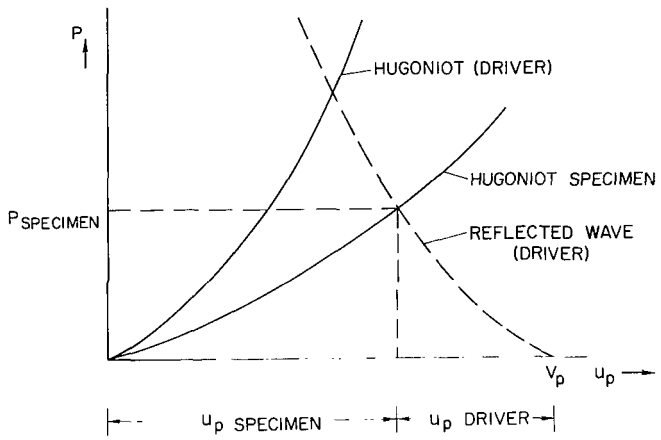

Figure 2.- Graphical impedance match solution for determining the peak pressure in target material for which the equation of state is known. The equation of state of the driver plate is known and only V_p is measured.

reflected driver's Hugoniot (at V_p) and the line with a slope of d_oU_s yields the achieved particle velocity and pressure in the material of interest. This commonly used technique was modified for the present work, where different materials were used for both projectile and target, but the equations of state for both materials were known. In this special case, it was necessary to measure only the impact velocity of the projectile and use the graphical technique to determine the peak pressure at the target/projectile boundary (fig. 2).

EXPERIMENTAL CONDITIONS

A. H. Jones, et al. (ref. 15) have described in detail projectile and target dimensions as well as the critical alinement of the target necessary to ensure one-dimensional flow for precise pressure determinations in the target specimen. The experimental setup described below was designed according to these specifications.

Projectiles

To date, the materials used as projectiles are Fansteel, Aluminum 2024, and Lexan. These materials have been chosen because of their established equations of state, their different densities, and their machinability. Relevant projectile characteristics are shown in table 1.

TABLE 1.- PROJECTILES

Material	Density, g/cm^3	Dimensions			Source of equations of state
		Length, mm	Diameter, mm	Weight, g	
Lexan	1.20	6	20	≈2.7	Isbell, et al. (ref. 18)
Aluminum 2024	2.78	3[a]	17	≈5.1	Thiel (ref. 19)
Fansteel 77	16.97	1.5[a]	17	≈9.8	Jones, et al. (ref. 15)

[a]In Lexan holder, 6 mm long × 20 mm diameter

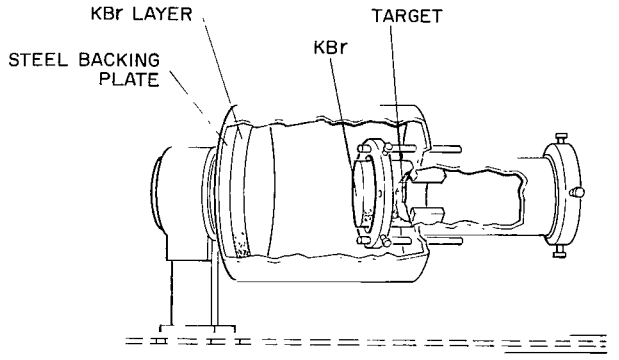

Figure 3.- Potassium bromide (KBr) pellet enclosing the mineral (quartz) target disk, mounted in the sample catcher of the shock range.

Target

The mineralogical targets were small quartz disks of 10-mm diameter and 1- to 2-mm thickness. The small disk was embedded in a block of pressed potassium bromide (KBr). Potassium bromide powder and the target were pressed together at 7000 kg/cm^2 and 350° C to form a solid pellet (fig. 3). The density of the KBr was 2.64 to 2.66 g/cm^3. During the embedding process, the KBr "flows" around the target disk and ensures a very tight fit. Salts other than KBr may be used, depending on their densities, for potting different minerals.

The KBr method serves several purposes. It assures that the whole target assembly is subjected to one-dimensional flow and reacts to the shock wave as a homogeneous medium. The shock wave passes through the quartz disk into the KBr without reflection or rarefaction. The impedances match ideally. In addition, KBr serves as a "holder" for the small target, thus increasing the efficiency of sample recovery. The target assembly is mounted in an aluminum container (fig. 3) having a 23-mm entrance hole for the projectile. The diameter of the entrance hole is as small as possible to ensure maximum sample retention. The shocked target material can be recovered quantitatively from the collected mixture of KBr and shocked quartz by dissolving the KBr in water.

Target Alinement

The most critical part of the experiment is to ensure that a planar shock wave passes through the target. The target surface and the surface of the impacting projectile must be parallel to ensure one-dimensional flow behind the shock front. Complicated mirror systems, wedge-shaped targets, electrical shorting pins, and other methods are normally used in equation-of-state work to measure the shock-wave velocity and the orientation of the shock front directly. The range at Ames was designed to minimize excessive tilt by optical and mechanical alinement procedures and to monitor actual projectile tilt by X-ray shadowgraph techniques in such a way that tilts greater than 1° could be recognized and the data discarded. Consequently, the pressures obtained from the selected data may deviate as much as ±3% from the established Hugoniot curves, but they are sufficiently precise for geological purposes. It should be noted that the existing equations of state themselves may contain uncertainties and the accuracy of the pressure calculations in this investigation depends on the accuracy of the established equations of state.

In order to ensure a planar shock wave, the projectile is photographed in flight by three X-ray flash units, arranged at angles of 60°. A grid

of fiducial wires is superimposed on the X-ray picture and a misalinement of more than 1° is readily recognizable (fig. 4). In addition, each shot requires the following target alinement procedure: A laser (or conventional light source with precisely centered apertures) is mounted at the breach end

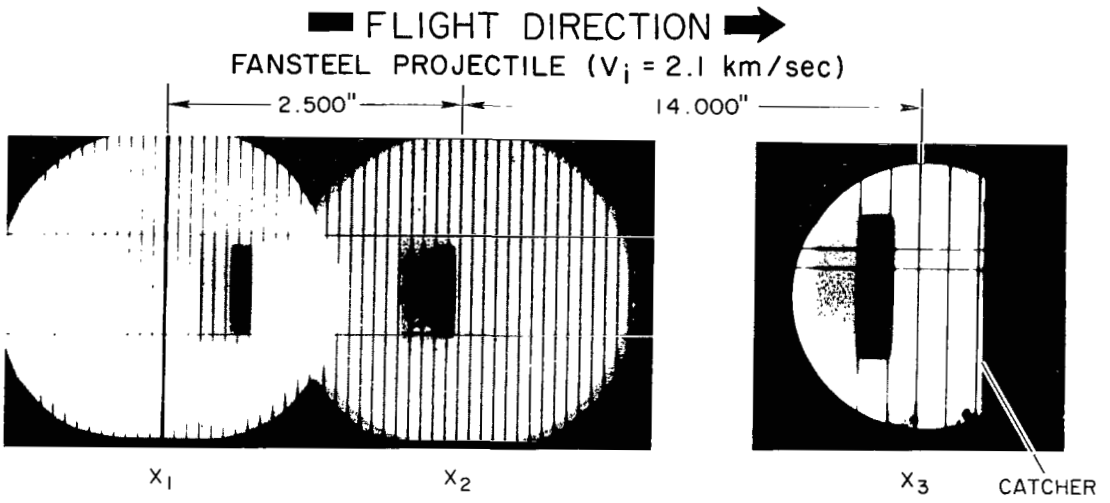

(a) A fansteel projectile in flight as photographed at sequential stations.

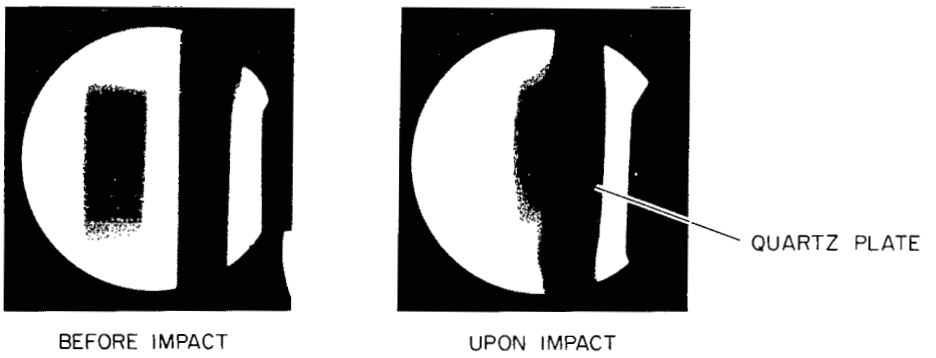

(b) Lexan projectiles immediately before and upon impact against a quartz plate.

Figure 4.- Flash X-ray shadowgraphs.

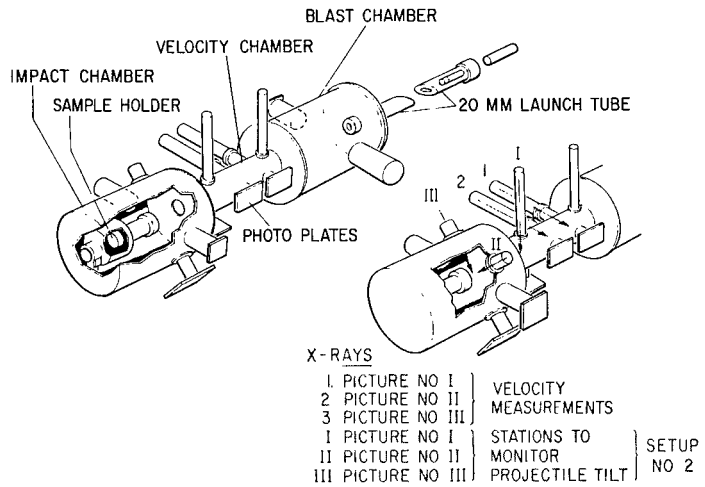

Figure 5.- Diagram of the shock range illustrating the locations of alining and triggering lasers and the flash X-ray tubes.

of the barrel and is directed through the whole range coaxial with the projectile's flight path (fig. 5). The laser beam strikes a small mirror, mounted on the target surface by adhesion of a thin grease film. The target is then adjusted by holding screws until the incident beam is reflected back on itself, producing an alinement accurate to less than 1/2°. The mirror is then carefully removed.

SHOCK RANGE DESCRIPTION

The basic parts of the shock range are a barrel and blast chamber, a velocity chamber, and an impact chamber. These are shown schematically in figure 5; the range and details are shown in figures 6 to 8, and the dimensions of the gun are given in the table.

Component	Length, cm	Outside diameter, cm
Launch tube	190	6.5 (20 mm ID)
Blast chamber	80	55
Velocity chamber	38	15
Impact chamber	55	50

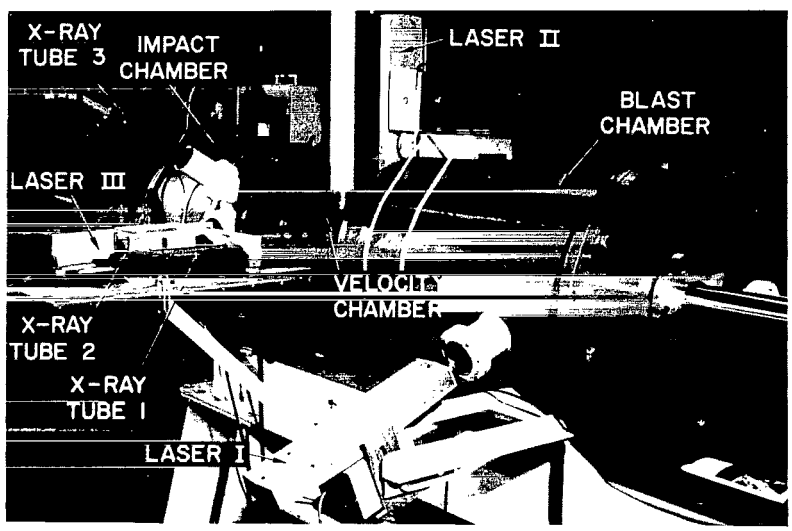

Figure 6.- Photograph of the impact shock range.

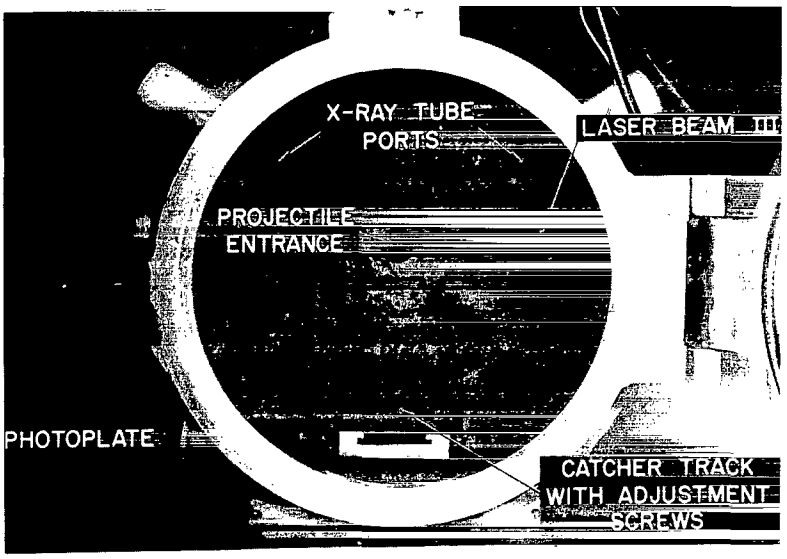

Figure 7.- Photograph of the impact chamber, looking uprange from the entrance door.

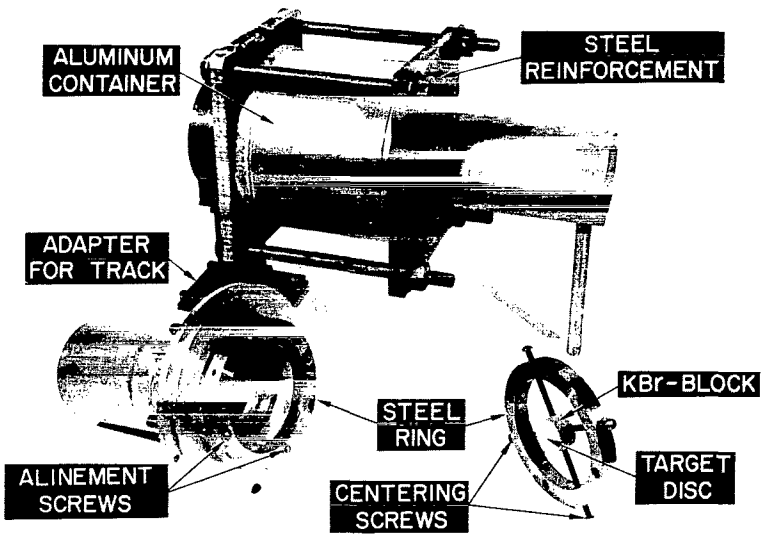

Figure 8.- Detail of the target holder-catcher system used in the impact shock range.

Loading Conditions

After the target is precisely alined, the proper powder charge and projectile are selected for the desired peak pressure in the target. Rough estimates of the expected projectile velocity are extrapolated from an

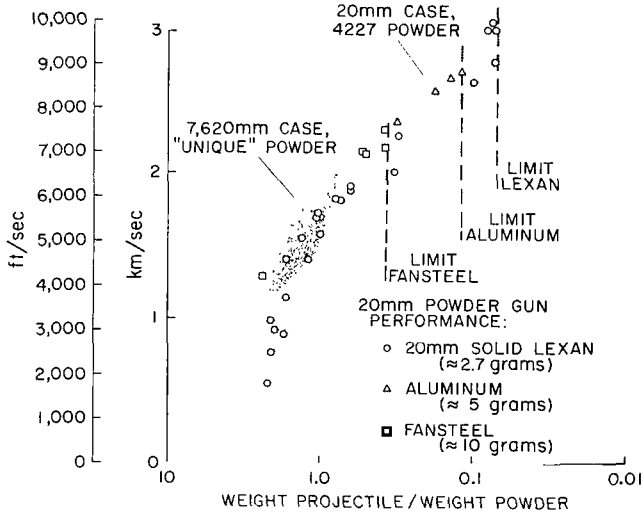

Figure 9.- Performance of the shock range gun. Velocity of the projectile as a function of the ratio projectile weight:powder weight for different cartridge cases and powder types.

empirical diagram (fig. 9). "DuPont 4227" or "Hercules Unique" powders are used as propellants and are contained in a standard 20-mm Navy case (M 103) or in a 300 Weatherby magnum cartridge (7.62-mm diameter), depending on the velocity desired. The projectile is hand loaded directly into the barrel and the loaded cartridges are placed behind it, either directly by means of a Mann action (20-mm caliber) or by a modified commercial 300 Weatherby rifle action with proper adaptor. The whole range is then evacuated to an air pressure of $1.5\text{-}2.0\times10^{-4}$ torr. The charges are ignited either directly by a high voltage pulse (20-mm caliber) or by a normal mechanical firing pin triggered with a solenoid attached to the rifle action (7.62-mm caliber).

Firing Sequence

The electric firing pulse to the gun also initiates simultaneously three 10-megacycle time-interval meters. The projectile is launched and travels through the barrel. Immediately after leaving the muzzle, the projectile interrupts the beam of a continuous He/Ne laser focused on a silicon planar pin photodiode. The resulting change in voltage output of the diode is amplified and stops the first counter L_1. The response time of the entire detector system is less than 1 μsec.

The model then travels through the blast chamber and enters the velocity chamber where it interrupts a second laser beam. The output change of the corresponding photodiode stops counter L_2 and simultaneously triggers time delay generators for discharging two X-ray flash tubes and starts counters X_1 and X_2. The delay time of each individual tube is preselected on the basis of predicted velocity so that the projectile will be positioned in the center of the field of view of each tube. The discharge pulses of X-ray tubes 1 and 2 (30-ns duration) stop counters X_1 and X_2. Two X-ray shadowgraphs of the driver plate are thus obtained with a superimposed grid of fiducial wires necessary to determine the precise location and orientation of the projectile (see fig. 4). The projectile then enters the impact chamber and interrupts a third laser beam, stopping counter L_3 and simultaneously starting counter X_3.

A third X-ray tube, mounted at an angle of 60° relative to the plane of tubes 1 and 2, takes a third picture of the projectile immediately before it enters the aluminum catcher and impacts the target. Counter X_3 is stopped by the discharge pulse of X-ray tube 3. From the laser beam photodiode systems and the discharge pulse of the X-ray tubes, six time intervals are

measured, each with an accuracy of ±0.5 μsec. This corresponds to a percentage accuracy of ±0.5 times the velocity in km/sec as determined from the L_1-X_3 time interval and distance. The corresponding distances are known to at least ±1 mm over a total distance of 97 cm (L_1-X_3), representing a negligible error in velocity determinations.

Gun Performance

Experience indicates that the maximum velocity obtainable with this powder gun is about 3.2 km/sec, the limiting factors being the mass of the projectile and the expansion velocities of the powder gases. The maximum velocities obtained with the facility described herein are 3.1 km/sec for solid Lexan slugs, 2.7 km/sec for aluminum, and 2.4 km/sec for Fansteel projectiles (fig. 9), reflecting the different masses of the projectiles (see table 1).

IMPACT METAMORPHISM EXPERIMENTS

Shocked quartz is well known from terrestrial meteorite craters, structures of suspected impact origin, and nuclear explosion craters (refs. 1, 2, 5-7, 10, 20-24). Petrographic and field geologic studies have made it possible to recognize various stages of the shock metamorphism of quartz. The stages (reflecting increasing shock intensities) are (1) quartz with planar elements (with various subclasses) formed by fracturing, slipping, and shearing along discrete lattice planes, (2) diaplectic quartz (subsolidus glass) resulting from complete destruction of the crystal lattice, and (3) lechatelierite (liquidus glass), resulting when shock temperatures (and pressures) are sufficiently high to cause fusion. The progressive change from stage 1 to 2 is reflected in the decrease of refractive indices, birefringence, and density, indicating a gradual breakdwon of the lattice.

Although the stages of metamorphism of quartz are well documented, there are few data relating specific shock features to exact peak pressures. Data obtained from experiments with single quartz crystals prior to this study are listed in table 2.

TABLE 2

Pressure, kb	Density, g/cm^3	Refractive index	X-ray pattern	Author, date, and remarks
250	2.65	Not measured	Alpha SiO_2	Wackerle (1962, ref. 25), planar shock
350	2.64	↓	Broadened lines	DeCarli and Jamieson (1959, ref. 26), planar shock
360	2.22	1.46	Amorphous	DeCarli and Jamieson (1959, ref. 26), convergent shock
500	2.204	Not measured	↓	Wackerle (1962, ref. 25), planar shock
600	2.22	1.46	↓	DeCarli and Jamieson (1959, ref. 26), planar shock

Since quartz is one of the most common rock-forming minerals and so few quantitative studies have been made of the shock metamorphism of quartz, the first experiments with this new range were conducted with this mineral.

This study has shown that it is very important to know the orientation of the propagating wave front with regard to the crystal lattice for purposes of geological interpretation. Therefore, the crystallographic orientation of the target is continuously monitored during fabrication of the small target disk by a Laue Polaroid X-ray camera. The accuracy of the plate's orientation is ±1°. Plates parallel to {0001}, {10$\bar{1}$0}, and {10$\bar{1}$1} have been shock loaded. The equation-of-state data of Wackerle (ref. 25), Ahrens and Gregson (ref. 27), and Fowles (ref. 28) were used to calculate the pressures in the quartz target (fig. 10). However, these data were obtained with quartz plates oriented with respect to rectangular engineering coordinates X, Y, Z (X = {2$\bar{1}\bar{1}$0}, Y = {01$\bar{1}$0}, Z = {0001}). In this study pressures generated in targets in the {0001} direction were calculated from the Z cut ({0001}) equation of state, introducing no error. Pressures generated in {10$\bar{1}$0} and {10$\bar{1}$1} directions were calculated using the X cut ({2$\bar{1}$$\bar{1}$0}) equation of state and represent the best approximations possible. Precise determinations of error for the computed pressures are not possible, but best estimates suggest that pressures calculated for {10$\bar{1}$0} directions are reasonably accurate, and that pressures calculated for the {10$\bar{1}$1} may be of the order of 5 percent low.

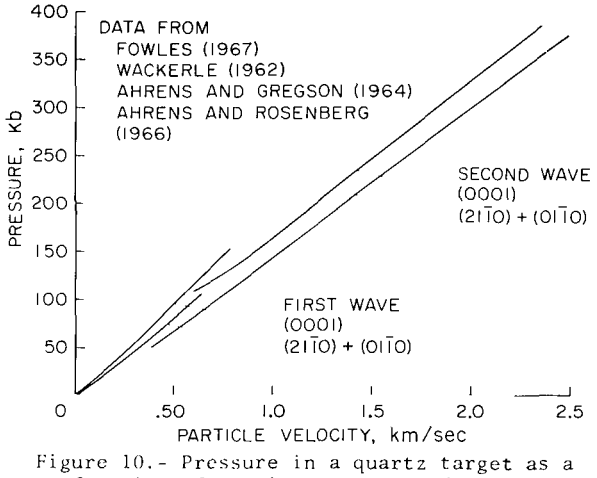

Figure 10.- Pressure in a quartz target as a function of particle velocity for different crystallographic orientations.

Results of the mineralogic studies of shocked quartz (ref. 29) are summarized here. The experiments at progressively higher pressures have confirmed the sequence of stages of progressive shock metamorphism recognized by petrographers, quartz with cleavage → quartz with planar features → diaplectic quartz, and have placed the various stages within the continuum in a pressure framework.

Cleavage (fig. 11(a)) as used here includes cleavage and faults of Carter (ref. 24). Cleavages are defined in this paper as through-going, broad features (2-10μ), widely spaced one from another (≥ 20μ) with symmetrical extinction and symmetrical movement of the Becke lines when cleavage is oriented parallel to the microscope axis. Cleavage is produced by shock pressures as low as 50 kb and develops predominantly on crystallographic planes with high resolved shear stress. Shocks propagating perpendicular to {0001} and {10$\bar{1}$0} produce these structures parallel to the unit rhombohedron (fig. 12); shocks propagating perpendicular to {10$\bar{1}$1} yield cleavages parallel to base and prism. This suggests that the cleavages recognized in these experiments were produced by faulting and are not cleavages in the strictest sense (ref. 24).

(a) Experimentally produced cleavage in quartz.

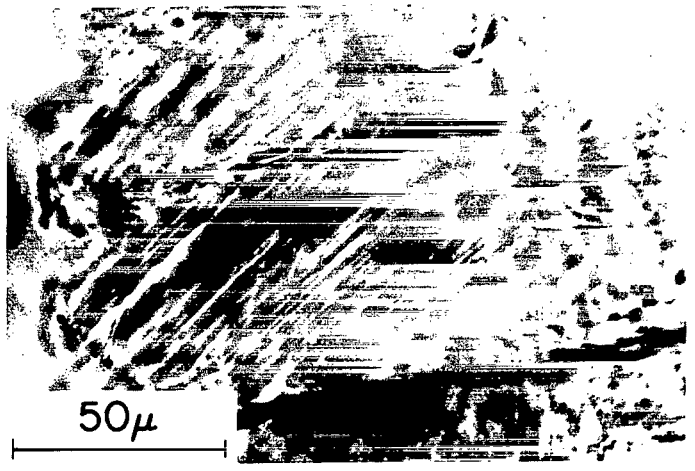

(b) Experimentally produced planar features in quartz.

Figure 11.- Deformation of single crystals of quartz by shock waves.

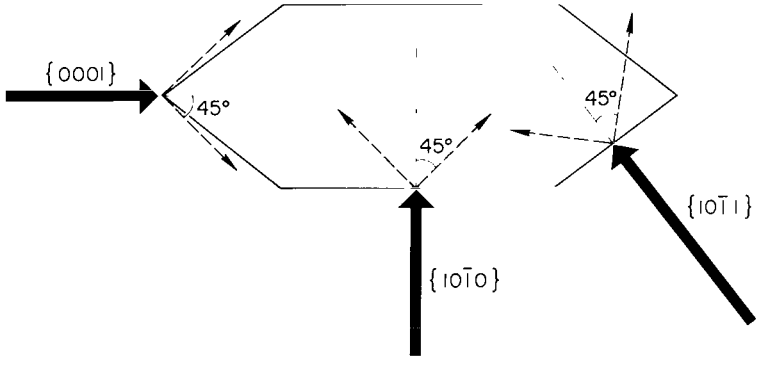

Figure 12.- Cross section through a quartz crystal with directions of impact (thick arrows) and directions of highest shear stress (dashed arrows).

Planar features (fig. 11(b)) include planar features and deformation lamellae of Carter (ref. 24). They are defined here as very thin planar structures ($\leq 2\mu$) that are very closely spaced (2-5μ) and occur in sets of five or more individuals and frequently in multiple sets. Planar features develop at pressures above 100 kb and cluster predominantly near $\{10\bar{1}3\}$, regardless of impact direction. At pressures above 160 kb, they are also strongly developed on $\{10\bar{1}2\}$, confirming the hypothesis of Robertson et al. (ref. 7) that the clustering of planar features around $\{10\bar{1}3\}$ indicates moderate shock pressures. Planar features parallel to {0001}, $\{11\bar{2}2\}$, $\{10\bar{1}1\}$, $\{11\bar{2}1\}$, $\{51\bar{6}1\}$, $\{21\bar{3}1\}$, and $\{10\bar{1}0\}$, or their symmetric equivalents, were also observed in quartz shocked to pressures in the 130-150 kb range, but because they form only rarely they do not appear suitable for describing the progressive shock metamorphism of quartz-bearing rocks.

Although the orientation of planar features is independent of the direction of propagation of the shock wave through the lattice, their frequency of development is orientation-dependent: grains shocked perpendicular to {0001} quite frequently have three to four different sets of planar features, whereas those shocked perpendicular to $\{10\bar{1}0\}$ and $\{10\bar{1}1\}$ even at higher stress levels rarely have as many as three different sets. It appears that the formation of planar features is possible only in the plastic region of the quartz Hugoniot equation of state. They are most likely produced by plastic gliding, but the precise mechanism of their formation is not yet known.

CONCLUDING REMARKS

The design and operation of this 20-mm powder gun facility provides a capability of shock loading rocks and minerals to precisely known pressures so long as their equations of state are known. Although calculated shock pressures deviate on the order of 15 percent from the established Hugoniot curves, this accuracy is sufficient for geological interpretations.

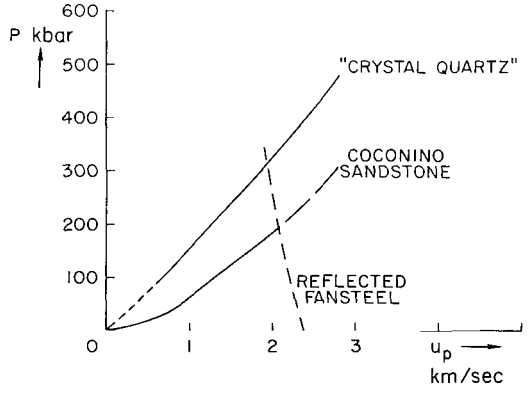

Figure 13.- Estimated maximum peak pressures in targets of quartz and sandstone which can be achieved with the impact shock range.

Because of the moderate projectile velocities that can be achieved with powder guns, the maximum shock pressures produced using Fansteel projectiles are low compared with those obtained by other experimental shock-loading techniques and meteorite impact events. Figures 13, 14, and 15 show estimated peak pressures in the Ames facility according to the shock wave data of Thiel (ref. 19) in various geological materials. Although these pressures are not sufficient to shock melt rocks and minerals, they produce a variety of solid-state reactions that are of special interest for the

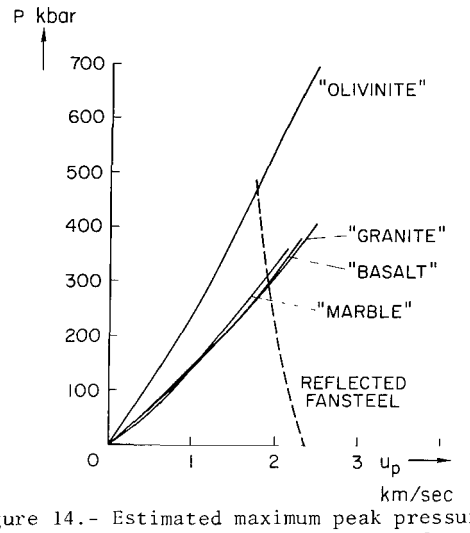

Figure 14.- Estimated maximum peak pressures which can be produced in targets of olivinite, granite, basalt, and marble with the impact shock range.

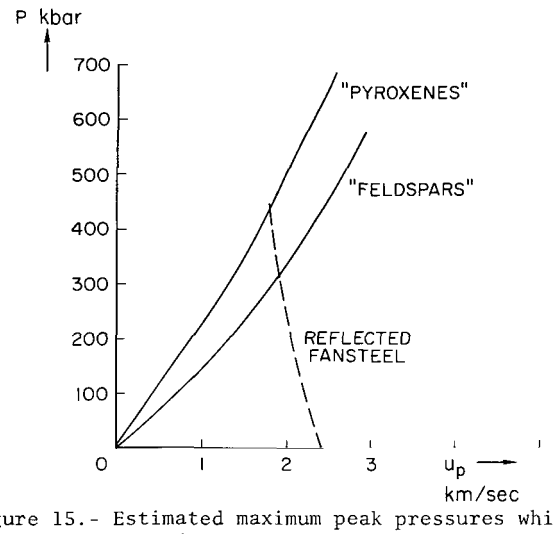

Figure 15.- Estimated maximum peak pressures which can be produced in targets of "pyroxene" and "feldspar" with the impact shock range.

understanding of impact metamorphism. A knowledge of the solid-state reactions in this pressure range would be of great value in the study and interpretation of impact craters.

At present, only few mineralogical data are available for shocked quartz and feldspars. The lack of controlled experiments on a variety of other rock-forming minerals, as well as mono- and heteromineralic rocks, quantitative evaluation of numerous petrographic observations of meteorites and of rocks from meteorite craters. Knowledge of the processes of shock metamorphism will aid in the interpretation of the history of returned lunar samples.

Ames Research Center
National Aeronautics and Space Administration
Moffett Field, Calif., 94035, Nov. 18, 1969

REFERENCES

1. Bunch, T. E.; Cohen, Alvin, J.: Shock Deformation of Quartz From Two Meteorite Craters. Bull. Geol. Soc. Am., vol. 75, no. 12, Dec. 1964, pp. 1263-1266.

2. Chao, E. C. T.: Shock Effects In Certain Rock-forming Minerals. Science, vol. 156, no. 3772, April 14, 1967, pp. 192-202.

3. Dence, M. R.: A Comparative Structural and Petrographic Study of Probable Canadian Meteorite Craters. Meteoritics, vol. 2, no. 3, Dec. 1964, pp. 249-270.

4. Dietz, Robert S.: Astroblemes. Scientific American, vol. 205, no. 2, Aug. 1961, pp. 50-58.

5. von Engelhardt, W.; and Stöffler, D.: Stages of Shock Metamorphism in Crystalline Rocks of the Ries Basin (Germany). Shock Metamorphism of Natural Materials, B. M. French and N. M. Short, eds., Mono-Book Corp., Baltimore, 1968, pp. 159-168.

6. French, Bevan M.: Sudbury Structure, Ontario: Some Petrographic Evidence for Origin by Meteorite Impact. Science, vol. 156, no. 3778, May 26, 1967, pp. 1094-1098.

7. Robertson, P. B.; Dence, M. R.; and Vos, M. A.: Deformation in Rock-Forming Minerals From Canadian Craters. Shock Metamorphism of Natural Materials, B. M. French and N. M. Short, eds., Mono-Book Corp., Baltimore, 1968.

8. Short, N. M.: Shock Processes in Geology. J. Geol. Education, vol. 15, no. 4, 1964, pp. 149-166.

9. Short, Nicholas M.: Effects of Shock Pressures From a Nuclear Explosion on Mechanical and Optical Properties of Granodiorite. J. Geophys. Res., vol. 71, no. 4, Feb. 15, 1966, pp. 1195-1215.

10. Stöffler, D.: Zones of Impact Metamorphism in Crystalline Rocks of the Nördlinger Ries Crater. Contr. Mineral. and Petrol., vol. 12, 1966, pp. 15-24.

11. Stöffler, D.: Deformation und Umwandlung von Plagioklas durch Stosswellen in den Gesteinen des Nördlinger Ries. Contr. Mineral. and Petrol., vol. 16, no. 1, 1967, pp. 51-83.

12. Deal, W. E.: Dynamic High Pressure Techniques. Modern Very High Pressure Techniques, Robert H. Wentorf, ed., Butterworths, Washington, 1962.

13. Doran, D. G.: Measurements of Shock Pressures in Solids, High Pressure Measurements, A. A. Giardini and Lloyd, eds., Butterworths Washington, D. C., 1963.

14. Duvall, G. E.: Concepts of Shock Wave Propagation. Bull. Seismol. Soc. Am., vol. 52, no. 4, 1962, pp. 869-893.

15. Jones, A. H.; Isbell, W. N.; and Maiden, C. J.: Measurement of the Very High Pressure Properties of Materials Using a Light Gas Gun. GM Defense Res. Labs. Tech. Rep. 65-84, 1965.

16. McQueen, R. G.; and Marsh, H. M..: Handbook of Physical Constants. S. P. Clark, ed., Series Memoir 97, Geol. Soc. of America, New York, 1966.

17. Rice, M. H.; McQueen, R. G.; and Walsh, J. M.: Compression of Solids by Strong Shock Waves. Solid State Physics, Frederick Seitz and David Turnbull, eds., vol. 6, Academic Press 1958, pp. 1-63.

18. Isbell, W. M.; Shipman, F. H.; and Jones, A. H.: Hugoniot Equation of State Measurements for Selected Geological Materials. GM Defense Res. Labs. Quarterly Progress Rep. No. 1, 1966.

19. van Thiel, M.: Compendium of Shock Wave Data. United States Atomic Energy Commission, Division of Technical Information, Lawrence Radiation Laboratory, University of California, Livermore, Calif., UCRL 50108, vol. 2, 1966.

20. Chao, E. C. T.; Shoemaker, E. M.; and Madsen, B. M.: First Natural Occurrence of Coesite. Science, 132, (#3421), July 22, 1960, pp. 220-222.

21. Chao, E. C. T., Fahey, J. J.; Littler, Janet; and Milton, D. J.: Stishovite, SiO_2, a Very High Pressure New Mineral From Meteor Crater, Arizona. J. Geophys. Res., vol. 67, no. 1, Jan. 1962, pp. 419-421.

22. von Engelhardt, W.; Hörz, F.; Stöffler, D.; and Bertsch, W.: Observations on Quartz Deformation in Breccias of West Clear Water Lake (Canada) and the Ries Basin (Germany). Shock Metamorphism of Natural Materials, B. M. French and N. M. Short, eds., Mono-Book Corp., Baltimore, 1968, pp. 475-483.

23. von Engelhardt, W.; Arndt, J.; Stöffler, D.; Müller, W. F.; Jeziorkowski, H.; Gubser, R. A.: Diaplektische Gläser in den Breccien des Ries von Nördlingen als Anzeichen fur Stosswellenmetamorphose. Contr. Mineral. and Petrol., vol. 15, no. 1, 1967, pp. 93-102.

24. Carter, N. L.: Dynamic Deformation of Quartz. Shock Metamorphism of Natural Materials, B. M. French and N. M. Short, eds., Mono-Book Corp., Baltimore, 1968, pp. 453-474.

25. Wackerle, Jerry: Shock-Wave Compression of Quartz. J. Appl. Phys., vol. 33, no. 3, March 1962, pp. 922-937.

26. De Carli, Paul S.; and Jamieson, John C.: Formation of an Amorphous Form of Quartz Under Shock Conditions. J. Chem. Phys., vol. 31, no. 6, Dec. 1959, pp. 1675-1676.

27. Ahrens, Thomas J.; and Gregson, V. G., Jr.: Shock Compression of Crustal Rocks: Data for Quartz, Calcite, and Plagioclase Rocks. J. Geophys. Res., vol. 69, no. 22, Nov. 15, 1964, pp. 4839-4874.

28. Fowles, Richard: Dynamic Compression of Quartz. J. Geophys. Res., vol. 72, no. 22, Nov. 15, 1967, pp. 5729-5742.

29. Hörz F.: Statistical Measurements of Deformation Structures and Refractive Indices in Experimentally Shock Loaded Quartz. Shock Metamorphism of Natural Materials, B. M. French and N. M. Short, eds., Mono-Book Corp., Baltimore, 1968, pp. 243-254.

NASA-Langley, 1970 —— 26 A-3181

NATIONAL AERONAUTICS AND SPACE ADMINISTRATION
WASHINGTON, D.C. 20546
OFFICIAL BUSINESS

FIRST CLASS MAIL

POSTAGE AND FEES PAID
NATIONAL AERONAUTICS AND
SPACE ADMINISTRATION

"The aeronautical and space activities of the United States shall be conducted so as to contribute . . . to the expansion of human knowledge of phenomena in the atmosphere and space. The Administration shall provide for the widest practicable and appropriate dissemination of information concerning its activities and the results thereof."

—NATIONAL AERONAUTICS AND SPACE ACT OF 1958

NASA SCIENTIFIC AND TECHNICAL PUBLICATIONS

TECHNICAL REPORTS: Scientific and technical information considered important, complete, and a lasting contribution to existing knowledge.

TECHNICAL NOTES: Information less broad in scope but nevertheless of importance as a contribution to existing knowledge.

TECHNICAL MEMORANDUMS: Information receiving limited distribution because of preliminary data, security classification, or other reasons.

CONTRACTOR REPORTS: Scientific and technical information generated under a NASA contract or grant and considered an important contribution to existing knowledge.

TECHNICAL TRANSLATIONS: Information published in a foreign language considered to merit NASA distribution in English.

SPECIAL PUBLICATIONS: Information derived from or of value to NASA activities. Publications include conference proceedings, monographs, data compilations, handbooks, sourcebooks, and special bibliographies.

TECHNOLOGY UTILIZATION PUBLICATIONS: Information on technology used by NASA that may be of particular interest in commercial and other non-aerospace applications. Publications include Tech Briefs, Technology Utilization Reports and Notes, and Technology Surveys.

Details on the availability of these publications may be obtained from:

SCIENTIFIC AND TECHNICAL INFORMATION DIVISION

NATIONAL AERONAUTICS AND SPACE ADMINISTRATION

Washington, D.C. 20546